Polyhedron 100 (2015) 114–120

Contents lists available at ScienceDirect

Polyhedron

journal homepage: www.elsevier.com/locate/poly

Electrochemical triggered O-atom transfer reaction in nitrocarbonyl rhenium(I) complexes: An IR spectroelectrochemical investigation

Sofía E. Domínguez, Florencia Fagalde *

INQUINOA-CONICET, Instituto de Química Física, Facultad de Bioquímica, Química y Farmacia, Universidad Nacional de Tucumán, Ayacucho 471, (T4000INI) San Miguel de Tucumán, Argentina

ARTICLE INFO

Article history:
Received 24 February 2015
Accepted 7 July 2015
Available online 11 July 2015

Keywords:
Polypyridyl rhenium(I)tricarbonyl
Nitrosyl complexes
IR spectroelectrochemistry
O-atom transfer reaction
Electrochemical oxidation of nitro-complexes

ABSTRACT

In previous work we proposed that polypyridylrhenium(I)tricarbonyl complexes coordinated to ion nitrite through its N-atom in CH_2Cl_2 solution could give nitrosyl complexes by electrochemical oxidation. In this work, we report for the first time by IR-spectroelectrochemical measurements that when $[Re^{I}(L)(CO)_3(NO_2)]$ oxidized to $[Re^{I}(L)(CO)_3(NO_2)]^+$ with L = 2,2′-bipyridine (bpy) and 4,4′-dimethyl-2,2′-bipyridine (dmb), an O-atom transfer reaction occurs triggered by electrochemical oxidation, leading to a complex with a $Re(CO)_2(NO)$ structure and releasing CO_2 by an intramolecular mechanism. Additionally, the Re-based oxidation and bipyridyl-based reduction of the nitro-complexes were investigated. The experimental results are in agreement with computational analysis calculated by DFT methods.

1. Introduction

Rhenium(I)tricarbonyl complexes have been extensively studied [1] because of its interesting photophysical and photochemical properties [2]. These complexes have led to applications such as sensors [3], molecular switches [4], building blocks in mixed-valent asymmetric dinuclear complexes [5] and catalysis [6,7]. Thus, for $[Re(diimine)(CO)_3(X)]^+$ complexes, electrochemical oxidations and reductions have been widely investigated, undergoing irreversible metal-based one electron oxidations and one-electron reductions that are centered on the α-diimine. Many of this reaction have been shown to be chemically reversible useful to reduce electrocatalytically carbon dioxide [8,9]. Also, there is interest in the development of novel radiopharmaceuticals with specific targets. In this sense, beyond employing tricarbonyl rhenium compounds, the potential use in radiopharmacy of various organometallic complexes have been investigated. In connection with this, the rhenium nitrosyl complexes are promissory [10,11] and could be useful agents to photo-delivery NO to biological targets [12]. On the other hand, biological and environmental relevance of NO has prompted an intense research towards nitrosyl coordination chemistry [13,14]. Also, the redox "non-innocent" behavior of coordinated nitrosyl makes it an interesting ligand for investigation [15]. The nitrite ligand has also very important physiological properties [16,17], and recently it was proposed as a "suspect ligand" [18]. Then, reactivity studies in rhenium carbonyl complexes with biological relevant ligands, such as NO_2^- and NO, are fundamental.

Regarding the reactivity of coordinated nitro ligand is interesting for the potential use as nitro based oxygen atom transfer catalysts [17,19]. Even more, the O-atom transfer reaction has been observed before for other complexes of several transition metals at room temperature and by thermal activation [9,20–24]. In these cases, intra or intermolecular mechanisms were proposed. In the first one, prior coordination of the ion nitrite occurs followed by O-atom transfer to adjacent bonded CO group, leading to spontaneous CO_2 loss and the formation of nitrosyl complexes. In the second case, the nucleophile NO_2^- attacks the bonded CO ligand leading to an ONOCO bonded moiety followed by elimination of CO_2 and transfer the NO ligand to the metal site.

Recently, we report the syntheses, characterization and photoinduced linkage isomerism of new polypyridyl rhenium(I)-tricarbonyl complexes with coordinated nitrite ion in the N- and O-binding mode [25]. In relation with this, from the waves observed in the cyclic voltammograms in CH_2Cl_2 using 0.1 M $TBAPF_6$ as supporting electrolyte, we proposed that nitrosyl complexes could be obtained in solution by oxidation of the nitro complexes, in concordance with previous reports for ruthenium and osmium nitro complexes [19,26].

In this work, we report for the first time in CH_2Cl_2 solution, that an O-atom transfer reaction occurs triggered by electrochemical

* Corresponding author.
E-mail address: ffagalde@fbqf.unt.edu.ar (F. Fagalde).

http://dx.doi.org/10.1016/j.poly.2015.07.010
0277-5387/

oxidation of complexes $[Re^{I}(bpy)(CO)_3(NO_2)]$, **(1)**, and $[Re^{I}(dmb)(CO)_3(NO_2)]$, **(2)** (with bpy = 2,2′-bipyridine and dmb = 4,4′-dimethyl-2,2′-bipyridine) leading to the oxidized species $[Re^{I}(bpy)(CO)_3(NO_2)]^{+}$ **(3)** and $[Re^{I}(dmb)(CO)_3(NO_2)]^{+}$ **(4)**. After that **(3)** and **(4)**, decomposed leading to a complex with a $Re(CO)_2(NO)$ structure and releasing CO_2 by an intramolecular mechanism. These measurements were done by cyclic voltammetry, UV–visible and by infrared spectroelectrochemistry. The experimental results were also in agreement with computational analysis by DFT methods.

2. Experimental

2.1. Materials, instrumentations and techniques

All chemicals used were analytical reagent grade and CH_2Cl_2 was anhydrous from Sigma–Aldrich. However, when we done the measurements (prior to the spectroelectrochemistry experiments) we have found that it was hydrated (see Section 3.1 and Fig. 1). The supporting electrolyte $TBAPF_6$ (*tetra-n*-butylammonium hexafluorophosphate) was dried at 150 °C for 24 h. The complexes $[Re^{I}(bpy)(CO)_3(NO_2)]$ **(1)**, (chem. anal. calc. for $C_{13}H_8N_3O_5Re$: C, 33.0; H, 1.7; N, 8.9. Found: C, 33.2; H, 1.7; N, 8.8%. ESIMS: *m/z* 495.99140 (M+Na)+), $[Re^{I}(dmb)(CO)_3(NO_2)]$ **(2)**, (chem. anal. calc. for $C_{15}H_{12}N_3O_5Re$: C, 36.0; H, 2.4; N, 8.4. Found: C, 35.9; H, 2.3; N, 8.2%. ESIMS: *m/z* 524.02270 (M+Na)+), and $[Re^{I}(dmb)(CO)_3(^{15}NO_2)]$ **(2′)** were prepared as previously described [25]. The oxidized complexes $[Re^{I}(bpy)(CO)_3(NO_2)]^{+}$ **(3)**, $[Re^{I}(dmb)(CO)_3(NO_2)]^{+}$ **(4)** and $[Re^{II}(dmb)(CO)_2(^{15}NO)(H_2O)]^{3+}$ **(6′)** and the reduced complexes $[Re^{I}(bpy)(CO)_3(NO_2)]^{\cdot -}$ **(7)**, $[Re^{I}(dmb)(CO)_3(NO_2)]^{\cdot -}$ **(8)** and $[Re^{0}(bpy)(CO)_3(NO_2)]^{-}$ **(9)** were obtained in situ by spectroelectrochemistry measurements.

Infrared spectra were obtained with a Perkin-Elmer Spectrum RX-1 FTIR spectrometer. An IR OTTLE cell [27] was employed equipped with CaF_2 windows and a Pt-minigrid working electrode, a Pt-minigrid as auxiliary electrode and Ag wire pseudo-reference electrode. Controlled potential electrolyses within the OTTLE cell were carried out using a *L.Y.P. electronic* potentiostat. Voltammetry experiments were carried out using BAS Epsilon EC equipment, with vitreous C as working electrode, Pt wire as auxiliary electrode, and Ag/AgCl (3 M NaCl) as reference electrode. In cyclic voltammetry experiments the concentrations were $c = 10^{-3}$ M for the complexes and 0.1 M for $TBAPF_6$. For spectroelectrochemistry experiments the concentrations of the complexes were $3{\cdot}10^{-3}$ M and 0.3 M for $TBAPF_6$. The IR spectroelectrochemistry measurements were done applying 100 mV steps potential, and when the initial spectrum began to change the steps were of 50 mV. After that, the potential at each step was maintained until the spectrum does not change anymore and then a new step was applied. The application of potential in small steps was done in order to avoid high electrolytic currents i_c and uncontrolled potential shifts due to a large ohmic potential drop i_cR ($\Delta E = E_{appl} - i_cR$) [28]. The range of potential employed were $0 < E < 2$V for the oxidation region and $0 < E < -1.8$ V for the reduction region. UV–Vis spectroelectrochemical experiments were performed in CH_2Cl_2 (0.1 M TBAH) using an *SEC-C* thin layer quartz glass spectroelectrochemical cell from *ALS*, with Pt gauze as working electrode, Pt wire as counter electrode and Ag/AgCl (3 M NaCl) as reference electrode. UV–Visible absorption spectra were recorded on a Varian Cary 50 spectrophotometer.

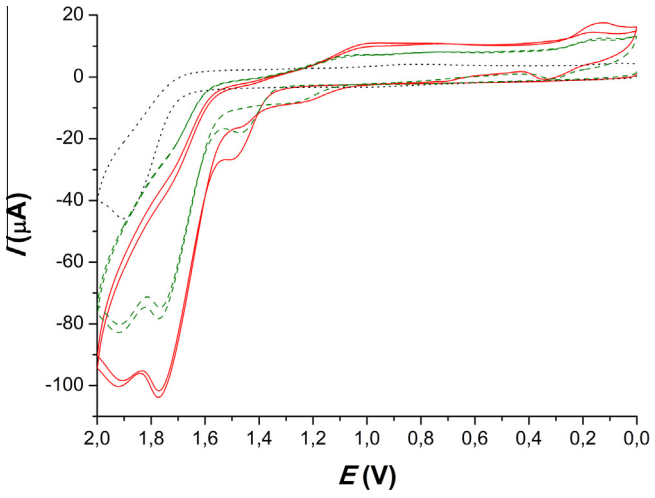

Fig. 1. Cyclic voltammetry at room temperature in CH_2Cl_2 – 0.1 M $TBAPF_6$ $v = 100$ mV s^{-1} for: supporting electrolyte (dotted black line), complex **(1)** (solid red line), and complex **(2)** (dashed green line). In complex **(1)** and **(2)** two subsequent scan are done. (Colour online.)

2.2. Quantum chemical calculations

The geometry optimizations and the vibrational frequencies were calculated by DFT methods using GAUSSIAN 03 program package [29]. Calculations employed the hybrid Perdew, Burke, Ernzerhof exchange and correlation functional (PBE1PBE) [30]. For H, C, N and O atoms, 6-311G** basis set were used. The Re atom was described by quasirelativistic effective core pseudopotential and corresponding set of basic functions [31]. The solvent was described by conductor-like polarizable continuum model (CPCM) [32].

3. Results and discussion

3.1. Cyclic voltammetry

3.1.1. Oxidation of *(1)* and *(2)* at different anodic potential

Fig. 1 shows cyclic voltammogram between 0 and 2 V for complexes **(1)** and **(2)** in $CH_2Cl_2/TBAPF_6$ obtained at a scan rate $v = 100$ mV s^{-1}. In both cases, as could be seen in the figure, the wave at 1.9 V corresponds to the oxidation of water present in the solvent of the supporting electrolyte as described in 2.1. As discussed previously for complexes **(1)** and **(2)** [25], the cyclic voltammogram shows three oxidation waves. The first one around 1.5 V which was previously assigned to the couples Re^{II}/Re^{I}, a second one irreversible at around 1.8 V and the third one corresponding to a reversible reduction at $E_{1/2} = 0.24$ V and attributable to the reversible nitrosyl couple formed. Furthermore, in the second cycle, the disappearance of the first oxidation wave at ~1.5 V involves the increasing of the wave assigned to the reversible nitrosyl couple formed, and a new irreversible band at 1.3 V corresponding to the couple Re^{II}/Re^{I} of the acuo-dicarbonyl-nitrosyl complex formed.

In order to confirm the generation of the nitrosyl couple both in complex **(1)** and **(2)**, we do the sweep between different potential oxidation ranges at two different scan rates. As could be seen in Fig. 2 for complex **(2)**, doing the sweep between 0 and 1.6 V at $v = 100$ mV s^{-1} and $v = 50$ mV s^{-1}, the wave at $E_{1/2} = 0.24$ V assigned to the nitrosyl group is not observed, only one wave appear corresponding to one electron oxidation of the rhenium(I). However, when the sweep is done between 0 and 1.84 V a new reversible wave appears at *ca.* 0.24 V, which can be assigned to the nitrosyl couple, as it is observed in Fig. 3. Therefore, the generation of the nitrosyl species is associated with the second oxidation process.

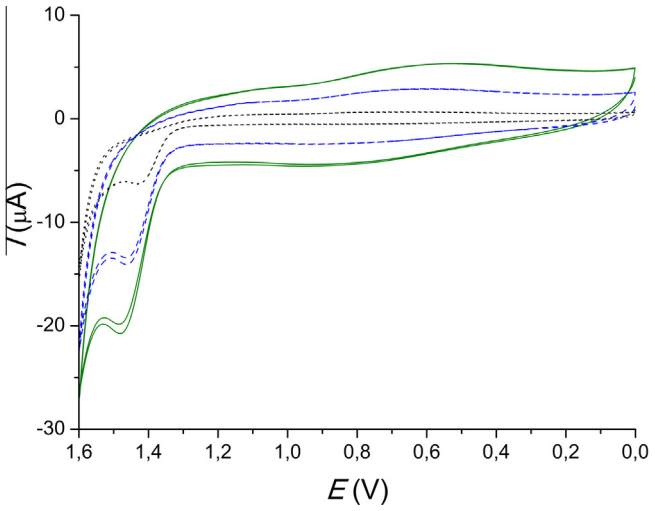

Fig. 2. Cyclic voltammetry at room temperature in CH_2Cl_2 – 0.1 M $TBAPF_6$ for complex **(2)** at: $v = 100$ mV s^{-1} (solid green line), $v = 50$ mV s^{-1} (dashed blue line), $v = 10$ mV s^{-1} (dotted black line). Range potential 0–1.6 V. Two subsequent scan are done in all cases. (Colour online.)

3.2. IR spectra and spectroelectrochemistry at different potentials

As discussed in previous work [25], both in KBr pellets as in CH_2Cl_2 solution, the IR spectra of complexes **(1)** and **(2)** shows characteristic vibrational modes between 1600 and 600 cm^{-1} corresponding to the polypyridyl ligands. The carbonyl frequencies ($\nu_{C\equiv O}$) in a facial configuration appear at 2031, 2023 and 1920 cm^{-1} for **(1)** and at 2029, 2021 and 1918 cm^{-1} for **(2)**. In addition, the antisymmetric and symmetric stretching modes for the nitro ligand ($\nu_{NO_2^-}$) coordinated to the rhenium(I) appears at 1354 and 1322 cm^{-1} for **(1)** and at 1357 and 1322 cm^{-1} for **(2)**. The splitting observed in solution for the stretching frequencies of the carbonyl frequencies ($\nu_{C\equiv O}$) are probably due to the presence of two conformers of each complex with the nitro ligand in different rotation angles.

Table 1 collecte the values of relevant stretching frequencies in CH_2Cl_2 for complexes **(1)** and **(2)**, and for the oxidation and reductions products observed in this work.

Figs. 4 and 5 shows for complexes **(1)** and **(2)** the IR spectroelectrochemistry in the carbonyl stretching frequencies region after applying a potential corresponding to the first oxidation process. The carbonyl stretching bands ($\nu_{C\equiv O}$) move to higher frequencies in the formed oxidized complexes $[Re(bpy)(CO)_3(NO_2)]^+$ **(3)**, and $[Re(dmb)(CO)_3(NO_2)]^+$ **(4)**. However, the small shift observed ($\Delta\nu \sim 9$ cm^{-1}) indicates that in these cases the first oxidation is localized mostly on the NO_2^- ligand instead of the oxidation of Re(I) to Re(II), which would result in much larger shift.

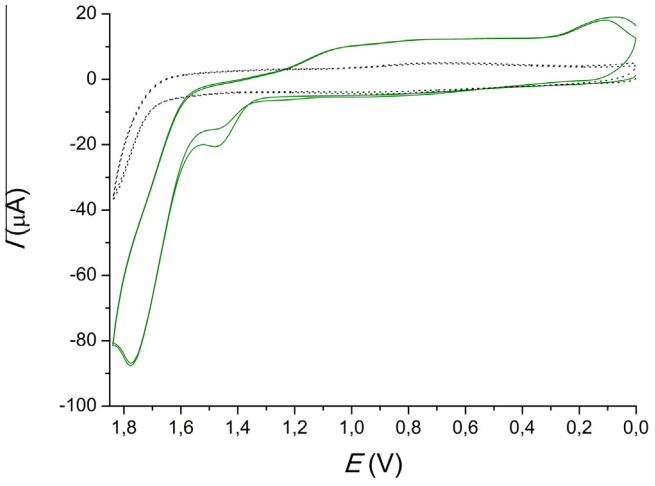

Fig. 3. Cyclic voltammetry at room temperature in CH_2Cl_2 – 0.1 M $TBAPF_6$ $v = 100$ mV s^{-1} for: supporting electrolyte (dotted black line), complex **(2)** (solid green line). Range potential 0–1.8 V. Two subsequent scan are done for complex **(2)**. (Colour online.)

Table 1
Relevant stretching frequencies in cm^{-1} in CH_2Cl_2 for complexes **(1)**, **(2)** and oxidation and reductions products observed in this work.

Complex	ν (CO)	ν (NO)
$[Re^{I}(bpy)(CO)_3(NO_2)]$ **(1)**	2031, 2023, 1920	
$[Re^{I}(dmb)(CO)_3(NO_2)]$ **(2)**	2029, 2021, 1918	
$[Re^{I}(bpy)(CO)_3(NO_2)]^+$ **(3)**	2039, 2031, 1931	
$[Re^{I}(dmb)(CO)_3(NO_2)]^+$ **(4)**	2038, 2029, 1929	
$[Re^{II}(bpy)(CO)_2(NO)(H_2O)]^{3+}$ **(5)**	2127, 2069	1827
$[Re^{II}(dmb)(CO)_2(NO)(H_2O)]^{3+}$ **(6)**	2124, 2065	1828
$[Re^{II}(dmb)(CO)_2(^{15}NO)(H_2O)]^{3+}$ **(6′)**	2127, 2068	1800
$[Re^{I}(bpy)(CO)_3(NO_2)]^{\cdot-}$ **(7)**	2009, 1990, 1897(sh), 1877	
$[Re^{I}(dmb)(CO)_3(NO_2)]^{\cdot-}$ **(8)**	2006, 1984, 1867	
$[Re^{0}(bpy)(CO)_3(NO_2)]^{-}$ **(9)**	1988, 1861	

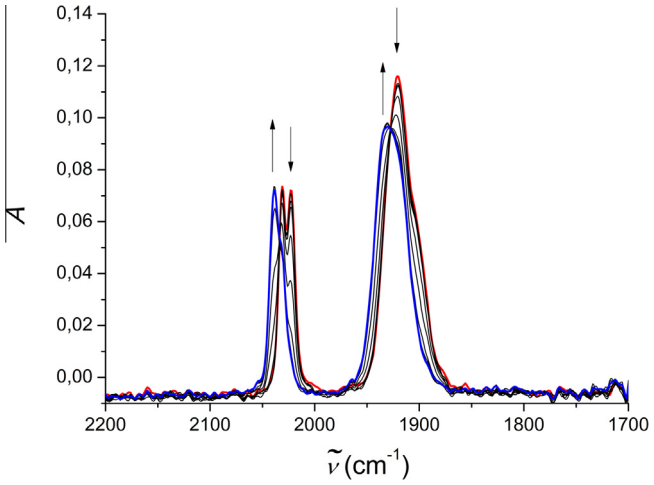

Fig. 4. ν_{CO} IR spectral changes following the first oxidation process for complex **(1)** (solid red line) leading to complex **(3)** (solid blue line). Arrows indicate whether the bands decrease or increase. (Colour online.)

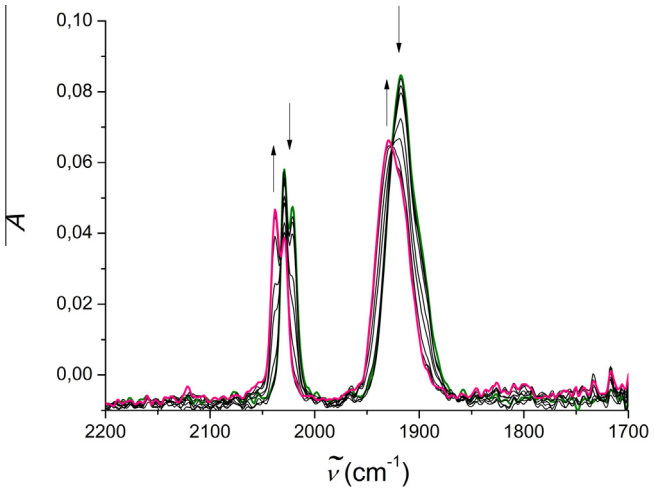

Fig. 5. ν_{CO} IR spectral changes following the first oxidation process for complex **(2)** (solid green line) leading to complex **(4)** (solid pink line). Arrows indicate whether the bands decrease or increase. (Colour online.)

As shown in Fig. 6a and Fig. 7a, at the beginning, when a higher potential corresponding to the second oxidation process is applied, small changes could be seen in the CO bands while the isosbestic points shift to lower energies. After that, complexes **(3)** and **(4)** began to decompose giving dicarbonyl nitrosyl complexes **(5)** and **(6)**. This conversion is carried out through a not identified intermediate prior to the O-atom transfer reaction as discuss in ref [8]. Thus, the bands corresponding to the C≡O stretching in complexes **(3)** and **(4)** disappear in the IR spectra with the concomitant apparition of three new bands at 2127, 2069 and 1827 cm^{-1} for complex **(5)** and at 2124, 2065 and 1828 cm^{-1} for complex **(6)** as shown in Figs. 6b and 7b.

The results are in agreement with literature [10] where these new bands are characteristic of the moiety $Re(CO)_2(NO)$ in dicarbonyl nitrosyl complexes. Furthermore, as seen in Figs. 6a and 7a and accordingly with experimental values, small changes appear in the region corresponding to the CO and NO band after applying a higher potential, principally in the axial CO bands of **(3)** and **(4)**, prior to the conversion to the dicarbonyl nitrosyl complexes of formulae $[Re^{II}(bpy)(CO)_2(NO)(H_2O)]^{3+}$ and $[Re^{II}(dmb)(CO)_2(NO)(H_2O)]^{3+}$.

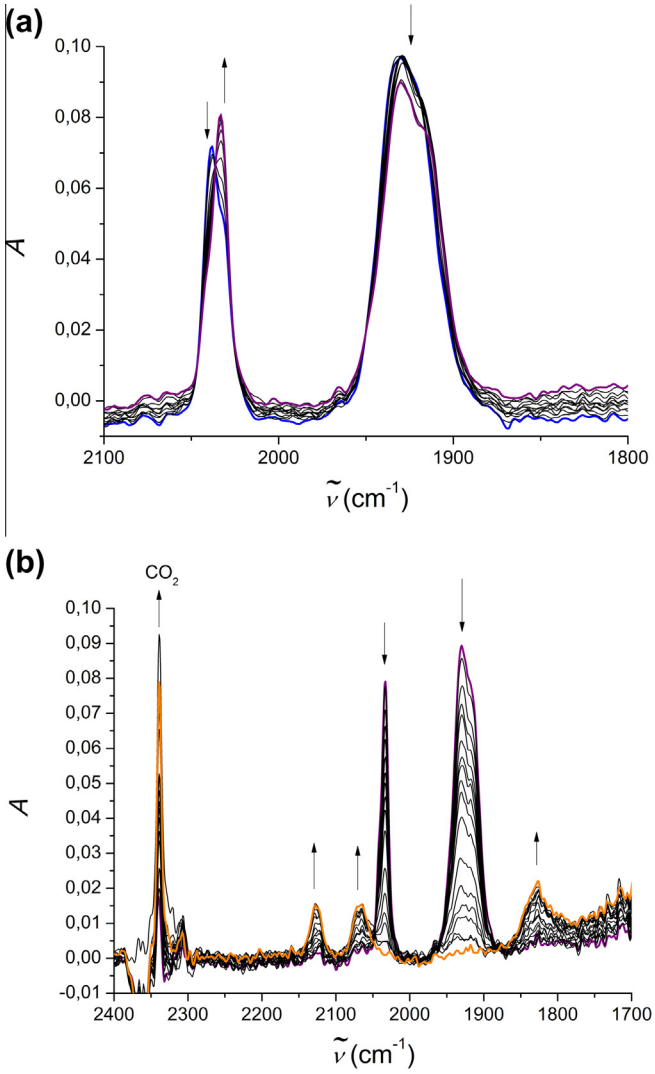

Fig. 6. IR spectral changes following the second oxidation process for complex **(1)**. (a) From complex **(3)** (solid blue line) to the formed intermediate (solid purple line). (b) Formation of complex **(5)** (solid orange line). Arrows indicate whether the bands decrease or increase. (Colour online.)

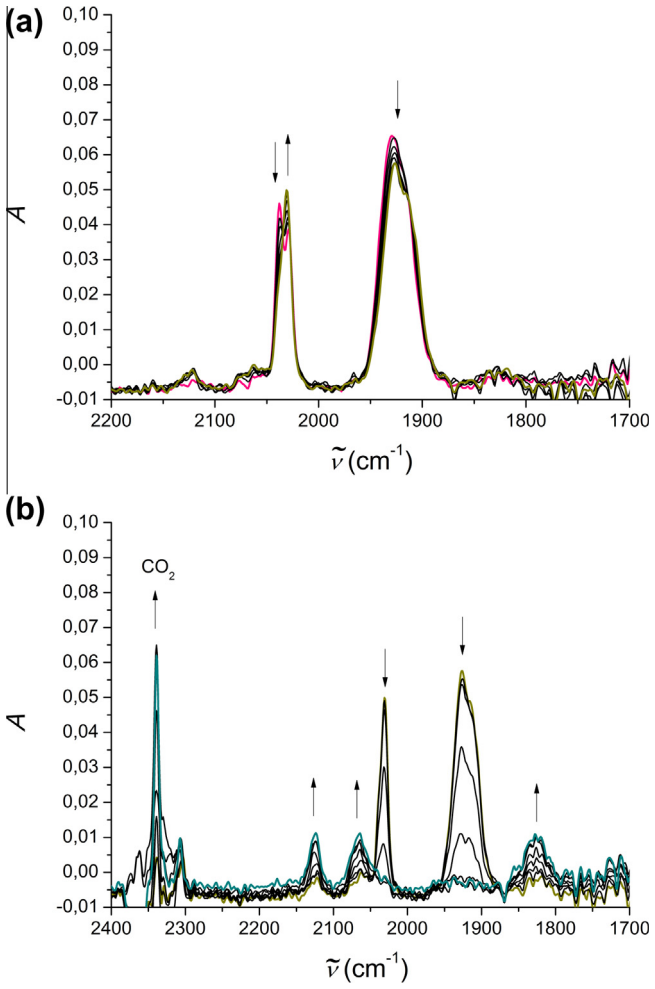

Fig. 7. IR spectral changes following the second oxidation process for complex **(2)**. (a) From complex **(4)** (solid pink line) to the formed intermediate (solid dark yellow line). (b) Formation of complex **(6)** (solid cyan line). Arrows indicate whether the bands decrease or increase. (Colour online.)

These new complexes formed by spectroelectrochemistry have two bands of $\nu_{C\equiv O}$ and one band of ν_{NO}, and would be the complexes *mer*-$[Re^{II}(bpy)(CO)_2(NO)(H_2O)]^{3+}$ for complex **(5)** and *mer*-$[Re^{II}(dmb)(CO)_2(NO)(H_2O)]^{3+}$ for complex **(6)** or its geometrical isomers *fac*-$[Re^{II}(bpy)(CO)_2(NO)(H_2O)]^{3+}$ and *fac*-$[Re^{II}(dmb)(CO)_2(NO)(H_2O)]^{3+}$, since it would derive from complex **(3)** and **(4)** by oxygen-atom transfer and subsequent loss of CO_2 by an intramolecular mechanism.

As shown in Table 1 and in Figs. 6 and 7, the bands assigned to the CO stretching modes (2127 and 2069 cm^{-1} for **(5)** and 2124 and 2065 cm^{-1} for **(6)**) shift to higher energies, because NO^+ ligand is better π-accepting than CO axial, then the π-backbonding to CO decreases in both complexes. On the other hand, as a result of oxidation of **(1)** and **(2)** at potential higher than the second oxidation process the bands around 1828 cm^{-1} corresponds to the formed NO^+ ligand.

To confirm this latter assignation, a potential higher than the second oxidation process was applied to the isotopic complex **(2′)** already synthesized in reference [25]. As observed in Fig. 8, for complex **(6′)**, the band corresponding to ^{15}NO appears at 1800 cm^{-1}, shifted 28 cm^{-1} to lower frequencies as it was expected for isotopic substitution, while the bands corresponding to the CO stretching modes appears at the same value as in **(2′)**.

What's more, in all cases, an intense band at 2339 cm^{-1} (Figs. 6b and 7b) corresponding to CO_2 is observed together with

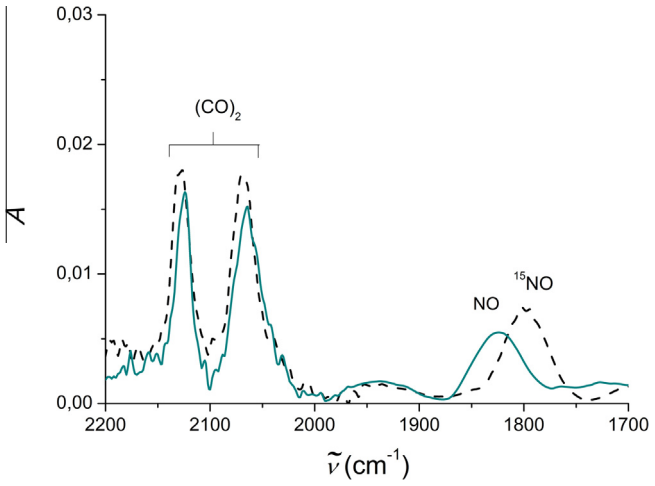

Fig. 8. IR spectra of formed complex **(6)** (solid cyan line) and the isotopic complex **(6′)** (dashed black line). (Colour online.)

the apparition of small bubbles in the cell as a result of the triggered O-atom transfer reaction in nitro carbonyl rhenium(I) complexes. In order to verify this assignment an IR spectrum of CO_2 in CH_2Cl_2 was measurement. Supporting information Fig. S1 shows an intense band at 2339 cm^{-1} corresponding to the stretching band of CO_2.

Additionally, changes observed in the IR spectroelectrochemistry spectrum for complexes **(3)** and **(4)** (Supporting information Figs. S2 an S3) in the OH stretching region, confirm that H_2O present in the supporting electrolyte might coordinates to the rhenium center in the sixth position. In addition, no changes were observed in the IR spectra for the first oxidation process (Supporting information Figs. S2a an S3a), contrary to what happens at potential higher than the second oxidation process, where the bands grow up and move to lower frequencies as a consequence of the coordination to the metallic center. These changes were associated with the lower possibility of the water molecules to present H-bonding due to the coordination and, moreover the coordination to the oxidized metallic center is favorable because the acuo ligand is good σ-donor and poor π-acceptor.

As shows in Eq. (1),

$$[Re(bpy/dmb)(CO_3)(NO_2)]^+ + H_2O \rightarrow [Re(bpy/dmb)(CO)_2(NO)(H_2O)]^{3+} + CO_2 + 2e^- \quad (1)$$

the mechanism of the reaction should be intramolecular, because the complexes have bonded to CO and NO_2, as proposed by Gordon et al. [33] and accordingly with Bullock et al. [8] where they describes the reactions of oxidized species of rhenium(I), through the formation of an hepta-coordinated species of Re(III). In base of the techniques used in this work, and in the absence of further mechanistic information an intramolecular oxidatively induced coupling of CO and NO_2^- ligands was demonstrated.

3.3. UV/Vis spectroelectrochemistry

As already discuss in Ref. [25], Fig. 9a show the spectroelectrochemical behavior of complex **(2)** at an applied potential E = 1.8 V in CH_2Cl_2, 0.1 M $TBAPF_6$, Δt = 0.4 min, after 5 min of measurements. Accordingly with the oxidation center in the Re(I), the bleaching of the MLCT band $d\pi(Re) \rightarrow \pi^*(dmb)$ is observed. Then the band at 360 nm began to decrease while a new shoulder appears at 325 nm. The shift of the isosbestic points at 250, 303 and 347 nm (Fig. 9b) to 247, 315 and 330 nm suggest that there is a relatively clean reaction following the oxidation and the pronounced sharp band at 325 nm indicates the presences of dmb in the product. On

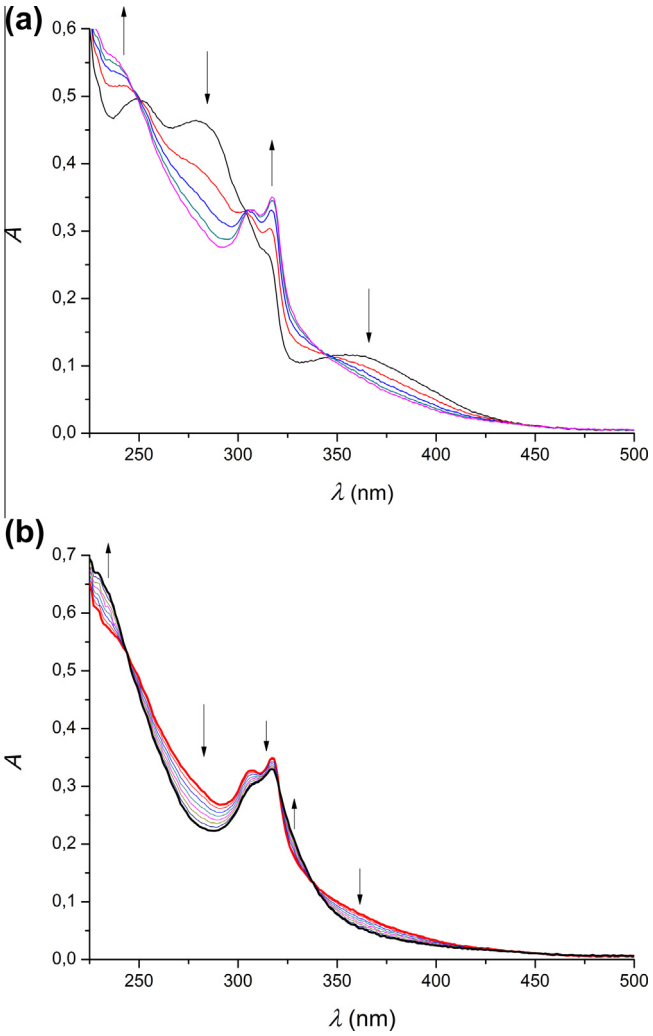

Fig. 9. Spectroelectrochemical behavior for complex **(2)** in 0.1 M $TBAPF_6$ in CH_2Cl_2 at an applied potential of E = 1.8 V, Δt = 0.4 min, (a) after 2 min, (b) after 5 min.

Table 2
DFT calculated stretching frequencies, in cm^{-1}, for complexes **(1)** and **(2)** and related complexes.

Complex	ν (CO)	(ν NO)
$[Re^I(bpy)(CO)_3(NO_2)]$ **(1)**	2112, 1998, 1997	–
$[Re^I(dmb)(CO)_3(NO_2)]$ **(2)**	2110, 1994, 1993	–
mer-$[Re^{II}(bpy)(CO)_2(NO)(H_2O)]^{3+}$ *mer*-**(5)**	2295, 2336	2062
mer-$[Re^{II}(dmb)(CO)_2(NO)(H_2O)]^{3+}$ *mer*-**(6)**	2334, 2293	2053
fac-$[Re^{II}(bpy)(CO)_2(NO)(H_2O)]^{3+}$ *fac*-**(5)**	2175, 2237	1991

the other hand, the disappearance of the broad band at about 275 nm which corresponding to intraligand $\pi \rightarrow \pi^*$ transitions of NO_2^- [25] suggest that complex **(4)** decompose to form the acuo-nitrosyl complex **(6)** by an O-atom transfer and subsequent loss of CO_2 by an intramolecular mechanism in agreement with IR-spectroelectrochemistry, and CV (Figs. 1, 7a and b, and Table 1).

3.4. DFT calculated IR spectra

Table 2 presented the values of calculated frequencies for complex **(1)** and **(2)**. Also were calculated the vibrational spectra for the complexes mer-$[Re^{II}(bpy)(CO)_2(NO)(H_2O)]^{3+}$ and mer-$[Re^{II}(dmb)(CO)_2(NO)(H_2O)]^{3+}$ and for the facial isomer of $[Re^{II}(bpy)(CO)_2(NO)(H_2O)]^{3+}$.

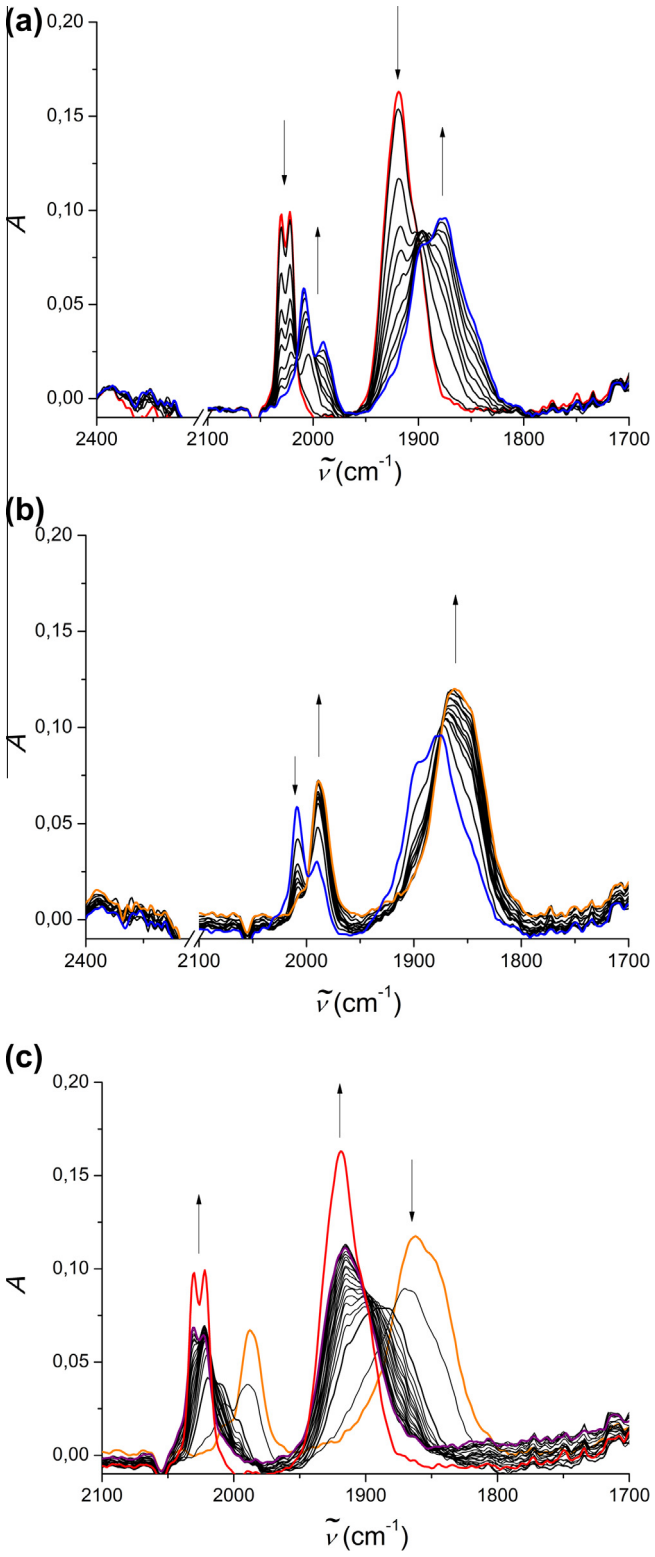

Fig. 10. (a) ν_{CO} IR spectral changes following the first reduction process for complex **(1)** (solid red line) leading to complex **(7)** (solid blue line). (b) IR spectral changes following the second reduction process, leading to complex **(9)** (solid orange line). **(c)** Recuperation of the original complex. Arrows indicate whether the bands decrease or increase. (Colour online.)

The agreement between experimental and calculated spectra used to be worse in CH_2Cl_2, due to the fact that CPCM model works better for more polar solvents [35]. Nevertheless, although the values of the frequencies are overestimated, it could be seen that the tendency is coherent with the experimental observations.

3.5. Reduction of [Re(bpy)(CO)$_3$(NO$_2$)] and [Re(dmb)(CO)$_3$(NO$_2$)]

As discuss in Ref [25], when a catodic potential is applied to polypyridines tricarbonyl Re(I) complexes at least one reversible reduction wave assigned to the reduction of the polypyridine appears. In CH_2Cl_2, 0.1 M $TBAPF_6$ for complex **(1)** and **(2)** the first reduction wave appears at $E_{1/2} = -1.32$ V and -1.40 V respectively, and even a second wave based in the couple Re^I/Re^0 is observed at -1.81 V for **(1)**.

For complex **(1)**, Fig. 10a shows the bipyridine-based reduction (complex **(7)**) and Fig. 10b the rhenium-based reduction (complex **(9)**). While for complex **(2)**, in Fig. 11a is presented the bipyridyl-based reduction (complex **(8)**).

As was observed previously for complexes of the type [Re(CO)$_3$(diimine)(L)] [34a] the reduction by one-electron is localized exclusively on the α-diimine ligand while in the subsequent one-electron reduction depending on the nature of L the Re center might also be involved [34b]. IR spectroelectrochemistry of reduced complexes **(7)** and **(9)** investigated in the CO stretching region, shows that bands corresponding to the CO stretching move to lower frequencies (Table 1) in the products. This is in accordance with the lower π-backbonding from Re(I) to the reduced bipyridine

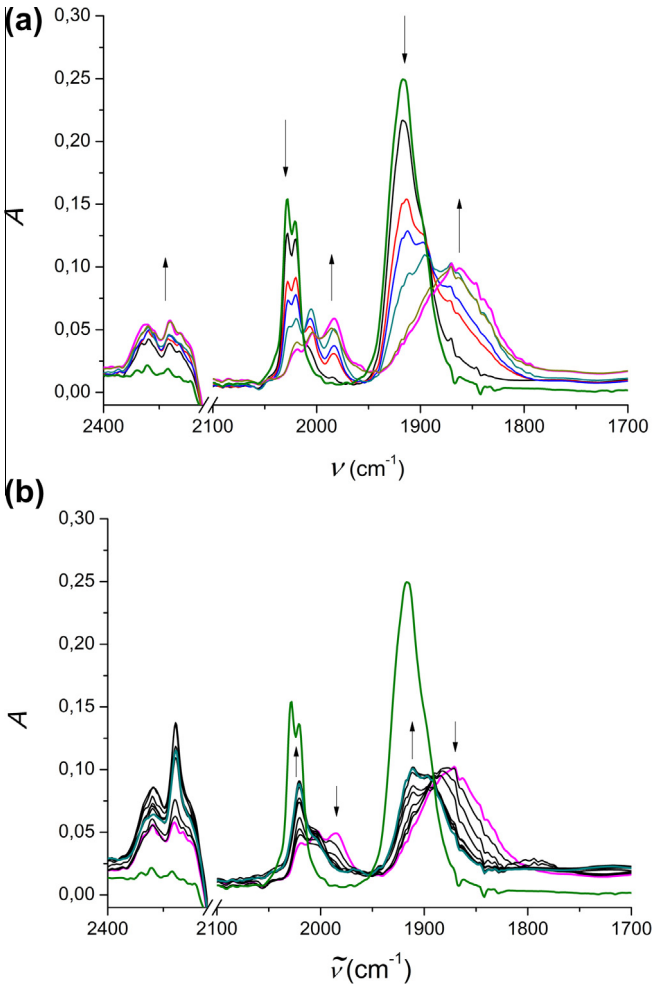

Fig. 11. **(a)** ν_{CO} IR spectral changes following the first reduction process for complex **(2)** (solid green line) leading to complex **(8)** (solid pink line). **(b)** Partial recovering of the initial complex. Arrows indicate whether the bands decrease or increase. (Colour online.)

ligand as a result of the higher Re → CO π-back bonding. Similar result was observed for complex **(2)** after applying cathodic potentials.

When a potential higher than the second wave based in the couple Re^{I}/Re^{0} was applied in complex **(1)**, there is no change. However, when a potential equal to 0 V is applied, it is observed the partial recuperation of the original complexes (Fig. 9c and Supplementary Fig. S4). Also it is observed a partial decomposition of the complex after re-oxidation and a band around 2339 cm^{-1}, which may correspond to oxidation of the CO released in the complex. While for complex **(2)** at potential higher than the first reduction wave (Fig. 10b), a band around 2339 cm^{-1} was observed which increases when the complex is reoxidized (Supplementary Fig. S5).

4. Conclusions

We have found for the first time that rhenium(II) nitrosyl-complexes could be obtained in solution by electrochemical oxidation of nitro-complexes, through an O-atom transfer process by an intermolecular mechanism. Also we report for the first time that this reaction occur by infrared spectroelectrochemical measurements with an OTTLE cell.

Acknowledgments

We thank Universidad Nacional de Tucumán (UNT), Consejo Nacional de Investigaciones Científicas y Técnicas (CONICET), and Agencia Nacional de Promoción Cientifica y Tecnológica (ANPCyT), all from Argentina, for financial support. F.F. is Member of the Research Career from CONICET. S.E.D. thanks CONICET for a graduate fellowship.

Appendix A. Supplementary data

Supplementary data associated with this article can be found, in the online version, at http://dx.doi.org/10.1016/j.poly.2015.07.010.

References

[1] Comprehensive Organometallic Chemistry III, vol. 5, Elsevier Ltd., 2007, pp. 868–886.
[2] A. Kumar, S.-S. Sun, A.J. Lees, Top. Organomet. Chem. 29 (2010) 1.
[3] (a) M. Cattaneo, F. Fagalde, N.E. Katz, Inorg. Chem. 45 (2006) 6884;
(b) M. Cattaneo, F. Fagalde, N.E. Katz, C.D. Borsarelli, T. Parella, Eur. J. Inorg. Chem. (2007) 5323.
[4] G. Pourrieux, F. Fagalde, I. Romero, X. Fontrodona, T. Parella, N.E. Katz, Inorg. Chem. 49 (2010) 4084.
[5] (a) J.H. MecchiaOrtiz, F.E. Moránvieyra, C.D. Borsarelli, I. Romero, X. Fontrodona, T. Parella, N.D. LisdeKatz, F. Fagalde, N.E. Katz, Eur. J. Inorg. Chem. (2014) 3359;
(b) F. Fagalde, M.E. García Posse, M.M. Vergara, M. Cattaneo, N.E. Katz, I. Romero, T. Parella, A. Llobet, Polyhedron 26 (2007) 17.
[6] P. Christensen, A. Hamnett, A.V.G. Muir, J.A. Timney, J. Chem. Soc., Dalton Trans. (1992) 1455.
[7] B. Probst, M. Guttentag, A. Rodenberg, P. Hamm, R. Alberto, Inorg. Chem. 50 (2011) 3404.
[8] J.P. Bullock, E. Carter, R. Johnson, A.T. Kennedy, S.E. Key, B.J. Kraft, D. Saxon, P. Underwood, Inorg. Chem. 47 (2008) 7880.
[9] B.F.G. Johnson, A. Sieder, A.J. Blake, R.E.P. Winpenny, J. Chem. Soc., Chem. Commun. (1993) 1345.
[10] (a) R. Schibli, N. Marti, P. Maurer, B. Spingler, M.L. Lehaire, V. Gramlich, C.L. Barnes, Inorg. Chem. 44 (2005) 683;
(b) M.L. Lehaire, P.V. Grundler, S. Steinhauser, N. Marti, L. Helm, K. Hegetschweiler, R. Schibli, A.E. Merbach, Inorg. Chem. 45 (2006) 4199.
[11] B. Machura, Coord. Chem. Rev. 249 (2005) 2277.
[12] P.C. Ford, J. Bourassa, K. Miranda, B. Lee, I. Lorkovic, S. Boggs, S. Kudo, L. Laverman, Coord. Chem. Rev. 171 (1998) 185.
[13] J.A. Olabe, L.D. Slep, Comprehensive Coordination Chemistry II, Vol. 1, Elsevier Ltd., 2003, pp. 603–623.
[14] F. Roncaroli, M. Videla, L.D. Slep, J.A. Olabe, Coord. Chem. Rev. 251 (2007) 1903.
[15] W. Kaim, Inorg. Chem. 50 (2011) 9752.
[16] P.C. Ford, Inorg. Chem. 49 (2010) 6226.
[17] J. Heinecke, P.C. Ford, Coord. Chem. Rev. 254 (2010) 235.
[18] F. Ehret, M. Bubin, S. Záliš, W. Kaim, Angew. Chem., Int. Ed. 52 (2013) 4673.
[19] R.A. Leising, S.A. Kubow, L.F. Szczepura, K.J. Takeuchi, Inorg. Chim. Acta 245 (1996) 167.
[20] B.F.G. Johnson, A. Sieker, A.J. Blake, R.E.P. Winpenny, J. Organomet. Chem. 475 (1994) 193.
[21] A. Sieker, A.J. Blake, B.F.G. Johnson, J. Chem. Soc., Dalton Trans. (1996) 1419.
[22] D.T. Doughty, R.P. Stewart Jr., G. Gordon, J. Am. Chem. Soc. 103 (1981) 3388.
[23] J.L. Hubbard, C.R. Zoch, W.L. Elcesser, Inorg. Chem. 32 (1993) 3333.
[24] G. Booth, J. Chatt, J. Chem. Soc. (1962) 2099.
[25] S.E. Domínguez, P. Alborés, F. Fagalde, Polyhedron 67 (2014) 471.
[26] (a) F.R. Keene, D.J. Salmon, J.L. Walsh, H.D. Abruña, T.J. Meyer, Inorg. Chem. 19 (1980) 1896;
(b) D.W. Pipes, T.J. Meyer, Inorg. Chem. 23 (1984) 2466.
[27] M. Krejčík, M. Daněk, F. Hartl, J. Electroanal. Chem. 317 (1991) 179.
[28] F.P.A. Johnson, M.W. George, F. Hartl, J.J. Turner, Organometallics 15 (1996) 3374.
[29] M.J. Frisch, G.W. Trucks, H.B. Schlegel, G.E. Scuseria, M.A. Robb, J.R. Cheeseman, J.A. Montgomery Jr., T. Vreven, K.N. Kudin, J.C. Burant, J.M. Millam, S.S. Iyengar, J. Tomasi, V. Barone, B. Mennucci, M. Cossi, G. Scalmani, N. Rega, G.A. Petersson, H. Nakatsuji, M. Hada, M. Ehara, K. Toyota, R. Fukuda, J. Hasegawa, M. Ishida, T. Nakajima, Y. Honda, O. Kitao, H. Nakai, M. Klene, X. Li, J.E. Knox, H.P. Hratchian, J.B. Cross, C. Adamo, J. Jaramillo, R. Gomperts, R.E. Stratmann, O. Yazyev, A.J. Austin, R. Cammi, C. Pomelli, J.W. Ochterski, P.Y. Ayala, K. Morokuma, G.A. Voth, P. Salvador, J.J. Dannenberg, V.G. Zakrzewski, S. Dapprich, A.D. Daniels, M.C. Strain, O. Farkas, D.K. Malick, A.D. Rabuck, K. Raghavachari, J.B. Foresman, J.V. Ortiz, Q. Cui, A.G. Baboul, S. Clifford, J. Cioslowski, B.B. Stefanov, G. Liu, A. Liashenko, P. Piskorz, I. Komaromi, R.L. Martin, D.J. Fox, T. Keith, M.A. Al-Laham, C.Y. Peng, A. Nanayakkara, M. Challacombe, P.M.W. Gill, B. Johnson, W. Chen, M.W. Wong, C. Gonzalez, J.A. Pople, Gaussian 03, Revision C.02, Gaussian Inc., Wallingford, CT, 2004.
[30] (a) P. Perdew, K. Burke, M. Ernzerhof, Phys. Rev. Lett. 77 (1996) 3865;
(b) C. Adamo, J. Barone, J. Chem. Phys. 110 (1999) 6158.
[31] (a) D. Andrae, U. Haeussermann, M. Dolg, H. Stoll, H. Preuss, Theor. Chim. Acta 77 (1990) 123;
(b) J.M.L. Martin, A. Sundermann, J. Chem. Phys. 114 (2001) 3408.
[32] M. Cossi, N. Rega, G. Scalmani, V. Barone, J. Comput. Chem. 24 (2003) 669.
[33] C.M. Gordon, R.D. Feltham, J.J. Turner, J. Phys. Chem. 95 (1991) 2889.
[34] (a) G.J. Stor, F. Hartl, J.W.M. van Outersterp, D.J. Stufkens, Organometallics 14 (1995) 1115;
(b) J.W.M. van Outersterp, F. Hartl, D.J. Stufkens, Organometallics 14 (1995) 3303;
(c) P. Christensen, A. Hamnett, A.V.G. Muir, J.A. Timney, J. Chem Soc. Dalton. Trans. 1455 (1992).
[35] A. Vlček Jr., S. Záliš, Coord. Chem. Rev. 251 (2007) 258.